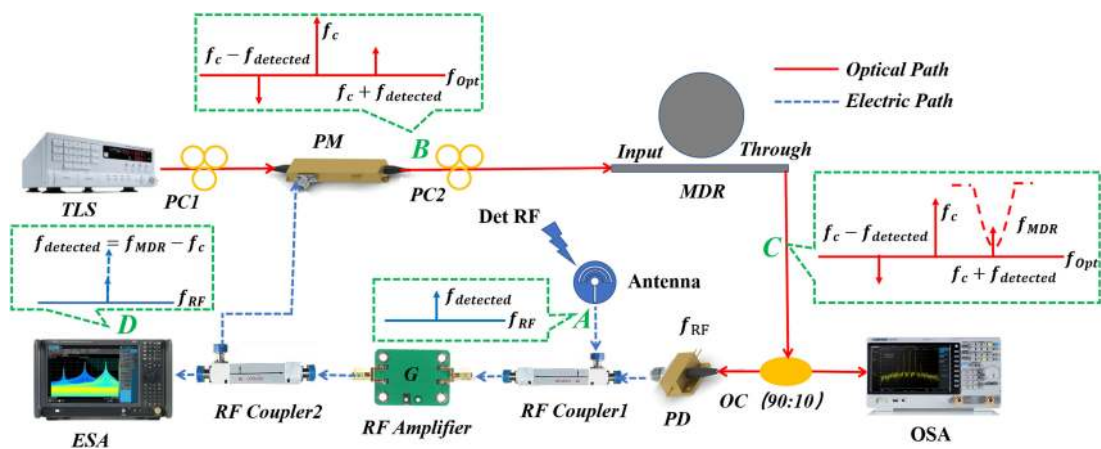


# Implementation of a Highly-Sensitive and Wide-Range Frequency Measurement Using a $\text{Si}_3\text{N}_4$ MDR-Based Optoelectronic Oscillator

Volume 11, Number 6, December 2019

Pengcheng Liu  
Pengfei Zheng  
Dongdong Lin  
Jing Li  
Xuemeng Xu  
Guohua Hu  
Binfeng Yun  
Yiping Cui



DOI: 10.1109/JPHOT.2019.2955928

# Implementation of a Highly-Sensitive and Wide-Range Frequency Measurement Using a Si<sub>3</sub>N<sub>4</sub> MDR-Based Optoelectronic Oscillator

Pengcheng Liu , Pengfei Zheng , Dongdong Lin, Jing Li, Xuemeng Xu, Guohua Hu , Binfeng Yun , and Yiping Cui 

Advanced Photonics Center, Southeast University, Nanjing 210096, China

DOI:10.1109/JPHOT.2019.2955928

This work is licensed under a Creative Commons Attribution 4.0 License. For more information, see <https://creativecommons.org/licenses/by/4.0/>

Manuscript received October 24, 2019; revised November 18, 2019; accepted November 22, 2019. Date of publication November 26, 2019; date of current version December 17, 2019. This work was supported in part by the National Key R&D Program of China under Grant 2018YFB2201800, in part by the National Natural Science Foundation of China under Grant 61601118, and in part by the Post-graduate Research & Practice Innovation Program of Jiangsu Province under Grant KYCX19\_0066. Corresponding author: Binfeng Yun (e-mail: ybf@seu.edu.cn).

**Abstract:** Microwave photonic technologies have been introduced for achieving broadband radio-frequency signal measurement. However, few of the proposed schemes mention the low-power radio-frequency signal detection, which stringently limits their practical applications in certain areas. In this paper, we designed and demonstrated a wideband low-power radio-frequency signal measurement system with optoelectronic oscillator. Here, the unknown radio-frequency signal matched the potential oscillation mode is allowable to be detected, amplified and estimated. The key component in the tunable optoelectronic oscillator is a silicon nitride micro-disk resonator with a very high Q-factor, which is utilized to achieve frequency selection as a microwave filter. A frequency measurement system range from 1 ~ 20 GHz with radio frequency power as low as -105 dBm, measurement errors of ±375 MHz and the maximum gain of 61.7 dB were realized experimentally

**Index Terms:** Micro-disk resonator, optoelectronic oscillator, frequency measurement.

## 1. Introduction

Frequency measurement has a great significance in the radar monitoring [1], wireless communication [2] and satellite remote sensing [3], in which the extremely low-power radio-frequency (RF) signal measurement is included as an essential survey. Due to the sufficiently large stream of data in those areas, challenges are brought to RF signal frequency measurements in terms of wide frequency range from a few megahertz to several tens of gigahertz. However, it is almost impossible to achieve the wideband frequency measurement due to the bandwidth limitation of pure electronic methods [4]. Microwave photonic technologies, which combine the RF engineering and optoelectronics, have the features of low loss, large bandwidth, immunity to electromagnetic interference (EMI), tunability, and reconfigurability for signal generation, transmission, processing and reception. Meanwhile, the characteristics of small size, light weight, and low power consumption put the photonic chip-integrated RF frequency measurement forward into a new scenario.

Recently, some microwave photonic frequency measurement approaches were proposed based on the principle of frequency-to-power mapping [5]–[8], frequency-to-time mapping [9]–[11], and

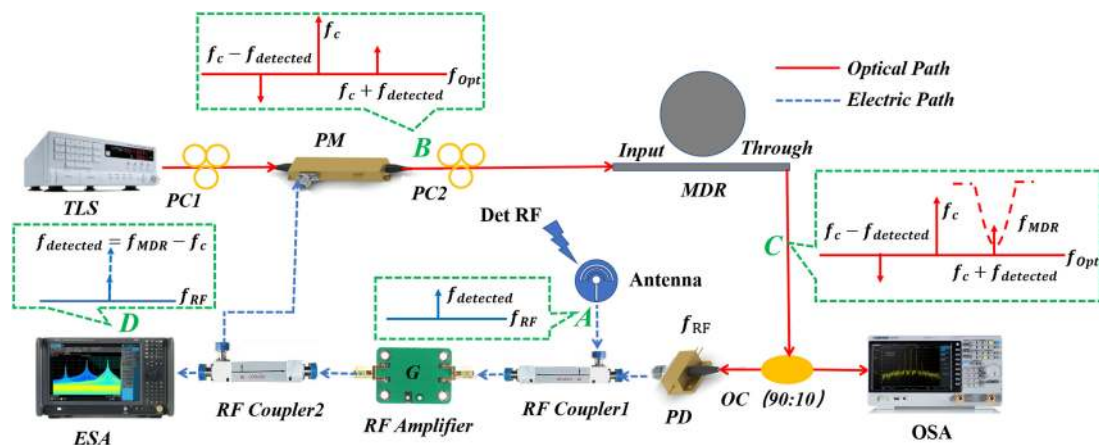


Fig. 1. The proposed link configuration of the frequency measurement system; TLS, tunable laser source; MDR,  $\text{Si}_3\text{N}_4$  micro-disk resonator; PC, polarization controller; OC, Optical coupler; OSA, optical spectrum analyzer; PM, phase modulator; PD, Photodetector; ESA, Electrical spectrum analyzer.

photonic channelization [12]–[14]. Among them, the frequency-to-power mapping scheme was realized based on an optical comb filter [5], the four-wave mixing (FWM) [6], a multichannel chirped fiber Bragg grating (FBG) [7], and a Mach–Zehnder interferometer (MZI) [8]. And the frequency-to-time mapping scheme was achieved by using a silicon-based swept filter [9], a dispersive medium [10], and a frequency shift loop [11]. Although the above-mentioned schemes can achieve the wideband RF frequency measurement, these methods are not concerned for measuring the RF signals with low power, which is always happen in receiver module. RF frequency measurement derived from optoelectronic oscillator (OEO) are implemented to enhance the RF power sensitivity. In Ref [12], a frequency measurement system by using a phase-shifted FBG-based tunable OEO was introduced to measure low-power RF signal. In the range of 1.5 ~ 5 GHz, the input RF power of  $-91$  dBm could be measured and measurement error of  $\pm 100$  MHz was achieved. In Ref [13], an OEO-based frequency measurement system using the effect of stimulated Brillouin scattering (SBS) was employed, which completed a frequency measurement range from 1 to 17 GHz, measured power sensitivity of  $-72$  dBm and maximum gain of 29 dB. Furthermore, frequency measurement using an integrated SBS tunable OEO was also reported [14], revealing a frequency measurement range from 1.5 to 40 GHz and the measured power sensitivity of  $-67$  dBm. However, optical pump power as high as 27 dBm is required to achieve the SBS. Moreover, the signal laser and the pump laser are introduced in the frequency measurement system, which may increase the measurement error derived from the wavelength jitter.

In this paper, a wideband frequency measurement system for measuring the extremely low-power RF signal is proposed with a  $\text{Si}_3\text{N}_4$  micro-disk resonator-based tunable OEO. When the frequency of the detected unknown RF signal matches the OEO's oscillation modes, the RF signal is selectively amplified by the OEO, then the frequency can be determined. The frequency measurement range, accuracy and power sensitivity of the RF frequency measurement system were analyzed. The experiment results show frequency measurement range of 1 ~ 20 GHz with power as low as  $-105$  dBm, measurement errors of  $\pm 375$  MHz, and maximum gain of 61.7 dB were realized. This scheme paves the way of monolithic silicon integration for RF signals frequency measurement.

## 2. Principle

The proposed link configuration of the frequency measurement system using a  $\text{Si}_3\text{N}_4$  micro-disk resonator (MDR) based OEO is shown in Fig. 1. The detected low-power unknown RF signal is fed into a phase modulator (PM) via the RF amplifier. Then the amplified RF signal is modulated

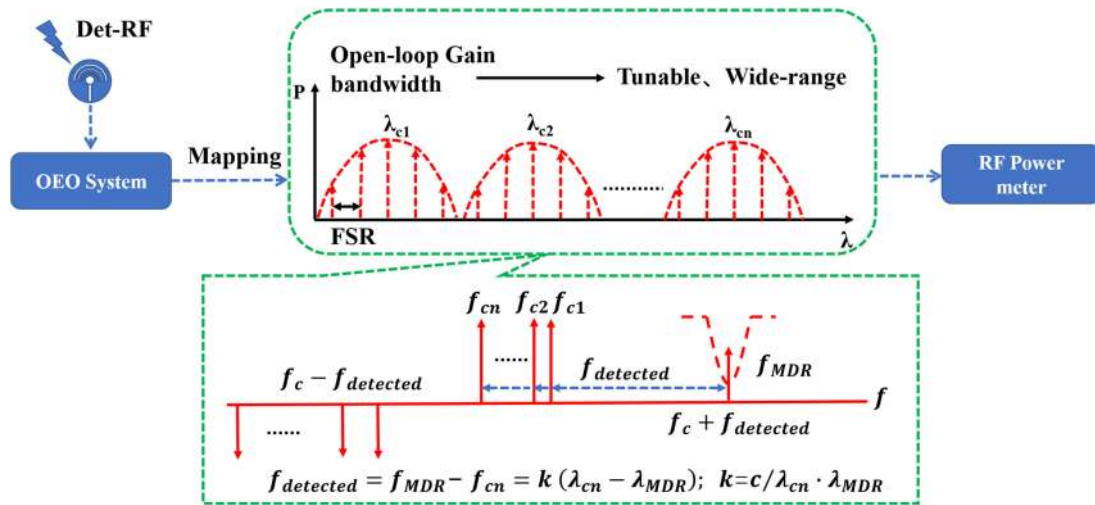


Fig. 2. The working principle of the OEO-based wide frequency measurement system,  $c$ : Speed of light.

onto the optical carrier with frequency  $f_c$  launched by a tunable laser (TLS). The optical double sideband modulation (ODSB) obtained by phase modulation is injected into an MDR notch filter with resonance frequency  $f_{MDR}$ . Then a RF passband filter response can be obtained by phase to intensity (PM-to-IM) conversion realized by signal beating in the photodetector (PD). The filtered RF signal then passes the RF coupler1, RF amplifier and RF coupler2 to the PM to form the close loop structure of the OEO. The polarization controller PC1 and PC2 are used to optimize the polarization dependent loss (PDL) of the PM and MDR, respectively. In addition, part of RF and optical signals are coupled out of the OEO loop through the RF coupler2 and optical coupler (OC) for monitoring.

At first, the  $\text{Si}_3\text{N}_4$  MDR-based OEO link need to be built according to the configuration of Fig. 1. By properly adjusting the laser power to keep the OEO's gain just below the oscillation threshold, when the OEO is most sensitive to an external unknown RF signal. Then the detected unknown RF signal will be fed into the RF coupler1's antenna receiving end of the OEO. Continuously frequency-tuning of the OEO can be realized by continuous sweeping the wavelength of the TLS. When unknown RF signal's frequency matches one of the potential OEO's oscillation modes, the RF signal will be detected, amplified and identified. On the contrary, if the frequency of unknown RF signal mismatches the potential oscillation modes, it will be attenuated and indistinguishable. Hence, the power sensitivity of the frequency measurement system can be intensely improved. The frequency measurement mechanism can be illustrated by the optical spectra at marked locations of the OEO link shown in Fig. 1. At location A, assume the antenna captures an unknown RF signal with frequency  $f_{detected}$ . At location B, the received low-power signal is sent into the PM via the RF amplifier and then modulated on the optical carrier launched by the TLS, whose frequency is  $f_c$ . Then an optical double sideband modulation (ODSB) with  $\pi$  phase shift between the  $\pm 1$ st order optical sidebands are generated. At location C, if the MDR notch filter's resonance frequency matches that of the +1st order optical sideband ( $f_c + f_{detected} = f_{MDR}$ ), the +1st optical sideband can be filtered and the PM-to-IM conversion is realized. At location D, the recovered and amplified signal with frequency  $f_{detected} = f_{MDR} - f_c$  can be obtained. Since the optical carrier's frequency  $f_c$  and the resonance frequency  $f_{MDR}$  of the MDR are known beforehand, the frequency  $f_{detected}$  of the detected RF signal can be obtained.

In addition to the power sensitivity of the system, the frequency measurement range is illustrated as shown in Fig. 2. Here the open-loop gain bandwidth is defined as the frequency range that link gain is greater than unity, which ensures OEO's oscillation [15]. And the  $\lambda_{cn}$  and  $f_{cn}$  are one-to-one correspondence between wavelength and frequency of the TLS. As mentioned above, only the RF signal with frequency matches one of the OEO's oscillation modes can be detected, amplified

and identified. In our design, a wide frequency measurement range is realized by using OEO's tunable open-loop gain spectrum, which can be achieved by sweeping the laser wavelength to reconfigure the frequency of the  $\text{Si}_3\text{N}_4$  MDR-based microwave photonic filter. To ensure at least one oscillation mode existing in the open-loop gain bandwidth, the relationship between the oscillation mode spacing and the minimum tuning wavelength spacing of the TLS must be considered. If the minimum tuning wavelength spacing of the TLS is greater than the OEO's oscillation mode spacing, it's indicative of at least one oscillation mode existing using the minimum tuning wavelength spacing of the TLS as the sweeping step of the measurement system. Conversely, in the case of the OEO's oscillation mode spacing is greater than the minimum tuning wavelength spacing of the TLS, the sweeping step of the measurement system must be greater than the oscillation mode spacing to ensure an oscillation mode present during the sweeping process. Thus, the sweeping step depends on the larger one between the oscillation mode spacing and the wavelength tuning spacing of the TLS. The frequency tuning range of the  $\text{Si}_3\text{N}_4$  MDR-based microwave photonic filter is confined by the wavelength difference of the adjacent  $\text{Si}_3\text{N}_4$  MDR's resonance dips. Hence, the frequency measurement range depends on the wavelength difference of the adjacent  $\text{Si}_3\text{N}_4$  MDR's resonance dips.

### 3. Experimental Results and Discussion

The relative experiment was carried out based on the link configuration shown in Fig. 1. The optical carrier was launched by the TLS (Santec WSL-100) whose the minimum tuning wavelength spacing of the TLS is 1 pm. In C-band (1525–1565 nm) 1 pm correspond to a bandwidth around of 125 MHz. The 3-dB bandwidth of the PM (Eospace) is 20 GHz. A RF amplifier (RFLNA-000200G27, 100 KHz ~ 20 GHz) was used to amplify the RF signal converted from the PD (Finisar, XPDV2120RA, DC ~ 50 GHz). The ESA (Keysight N9040B) was used to measure the magnitude of the output RF signals from the  $\text{Si}_3\text{N}_4$  MDR-based OEO.

As a key component in the system, the MDR was fabricated by the TriPleX waveguide technology [16]. The schematic of the MDR is shown in Fig. 3(a). The radius (R) of the MDR is 100  $\mu\text{m}$  and the gap is 1.05  $\mu\text{m}$ . The optical transmission spectra of the MDR was obtained by the Lightwave measurement system (Agilent 8164A), as shown in Fig. 3(b). Here the  $\Delta\lambda$  is defined as the wavelength difference between the resonance dips of the  $\text{Si}_3\text{N}_4$  MDR. And here the resonance dip with largest extinction ratio (ER) in the blue dot box was selected as the notch filter in our system. The measured  $\Delta\lambda$ , insertion loss and ER are 1.023 nm, 2.7 dB and 19 dB, respectively. Besides, the frequency measurement range of  $0 \sim \Delta\lambda/2$  (up to 64 GHz) can be obtained due to the optical double sideband modulation (ODSB) employed in the microwave photonic link, regardless the RF device performances. For achieving a spectrum with better resolution, the optical vector network analyzer (OVNA) based on the optical single sideband (OSSB) modulation link was carried out, and the spectra of the MDR can be obtained from the high precision vector network analyzer (VNA, Keysight N5242A) as shown in the Fig. 3(c). A 3-dB bandwidth of 312 MHz of the MDR is obtained. Comparing with the micro-ring resonator (MRR), the greater Q-factor can be obtained in MDR. And the greater Q-factor benefits for the oscillation mode selection of the OEO. Comparing with the desktop optical filter or the PS-FBG, the MDR-based notch filter can be applied for fully integrated frequency measurement systems.

To examine the operating characteristic of the proposed MDR-based OEO, the open loop gain spectra and the RF power spectrum were measured. As shown in Fig. 4, a perfect match is demonstrated between the open loop gain spectrum and the RF power spectrum at 10 GHz frequency.

To demonstrate the amplification ability, the level of  $-93$  dBm RF signals of  $f_1 = 11.656$  GHz and  $f_2 = 11.651$  GHz were fed into the system, respectively. The response spectra of the output signals are shown in Fig. 5(a). The tunable OEO's mode spacing or FSR is about 10 MHz, which is determined by the OEO loop length including the fiber length (15 m) and the coaxial cable length (5 m). As the OEO shows a 10 MHz FSR, this system is blind to many frequencies. Here, the OEO-based frequency measurement system is more suitable for photonic channelization frequency

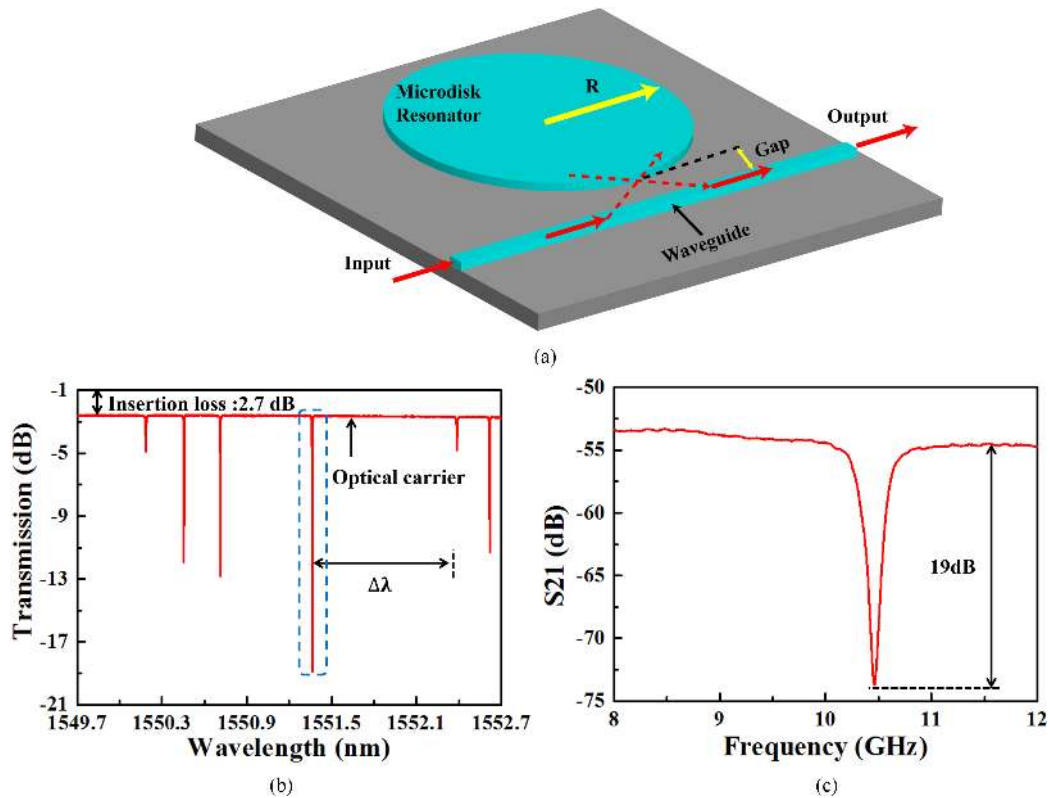


Fig. 3. (a) The structure of the MDR; (b) the measured optical transmission spectra of the MDR; (c) the detailed spectra of the MDR.

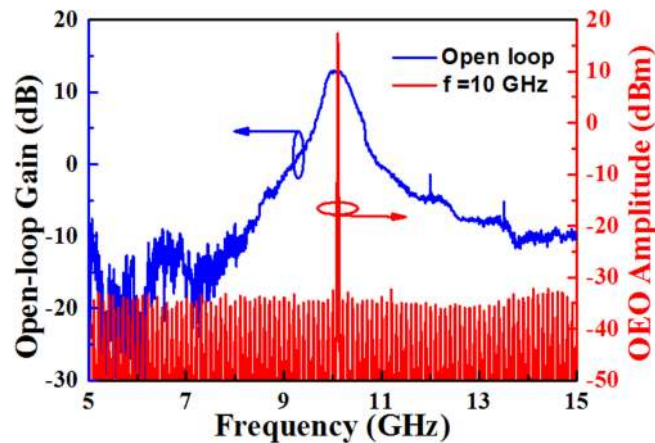


Fig. 4. The open loop gain spectra (blue) and the oscillation signal (red) at the frequency of 10 GHz (RBW = 3 MHz).

measurement. In addition, the loop delay of the OEO can be controlled by increasing or decreasing the loop length. By increasing the fiber length in the OEO system, the FSR of the OEO will be decreased and more frequencies can be caught. The output RF signal at matching the potential oscillation mode frequency  $f_1$  is amplified, while the signal at mismatching the oscillation mode frequency  $f_2$  is below the noise floor. In addition, for exploring the high-frequency characteristics of the frequency measurement system, the amplification ability for the RF signals at frequency

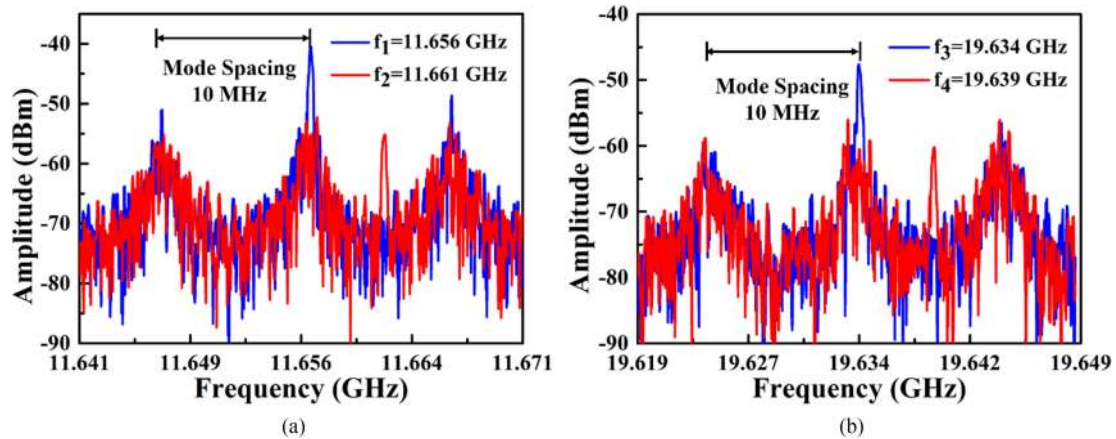


Fig. 5. OEO's output frequency response with the fed RF power of  $-93$  dBm at the frequency of (a)  $f_1 = 11.656$  GHz and  $f_2 = 11.651$  GHz; (b)  $f_3 = 19.634$  GHz and  $f_4 = 19.639$  GHz (RBW = 270 KHz).

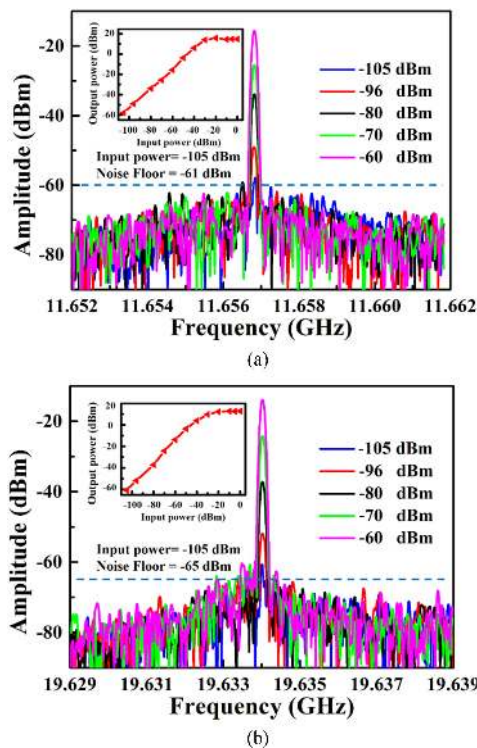


Fig. 6. Frequency spectra of the output signals with increasing input power at the frequency of (a) 11.656 GHz; and (b) 19.634 GHz (RBW = 91 KHz).

around 20 GHz was also measured. The level of  $-93$  dBm RF signals of  $f_3 = 19.634$  GHz and  $f_4 = 19.639$  GHz were fed into the system. The corresponding results are given in Fig. 5(b). The power of the RF signal with the frequency  $f_3$  matching the OEO's oscillation mode is amplified. On the contrary, the RF signal with the frequency  $f_4$  mismatching the oscillation mode cannot be distinguished from the noise floor.

The gain dynamic range and the measurement power sensitivity of the frequency measurement system were also investigated. The RF signals at frequency 11.656 GHz and 19.634 GHz with increasing power from  $-105$  to 0 dBm were injected into the system. As shown in Fig. 6(a), when

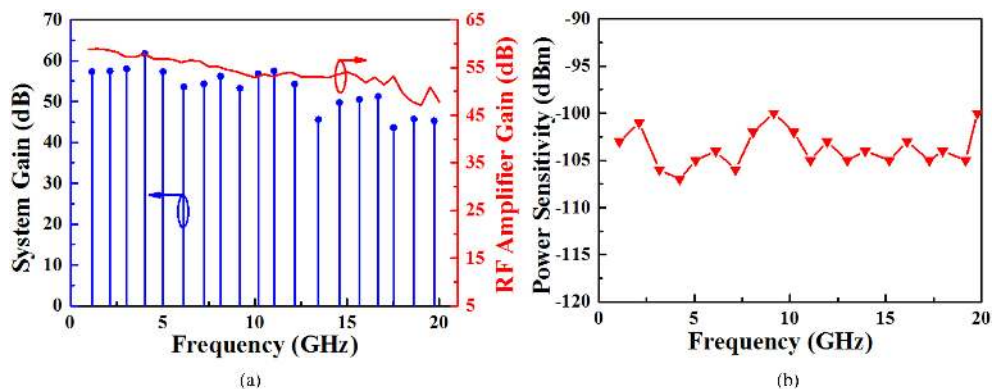


Fig. 7. (a) System gains (blue) and RF amplifier gains (red) at different RF frequencies and (b) the relationship between the sensitivity and frequency.

the input RF signal power is  $-105$  dBm, an output RF signal power of  $-58$  dBm and the noise floor power of  $-61$  dBm can be clearly observed in ESA. The measurement power sensitivity for 19.634 GHz is about  $-105$  dBm when the noise floor power is  $-65$  dBm as shown in Fig. 6(b). Therefore, the measurement power sensitivity reaches  $-105$  dBm, which is drastically improved than those in Ref [12]–[14]. The gain dynamic range is defined as the range between the lowest and highest detected RF power before OEO's saturation. As shown in the inset of Fig. 6, the OEO saturates when input RF power exceeds  $-30$  dBm, which means the gain dynamic range of the OEO system is close to 75 dB. Comparing the Fig. 6(a) with Fig. 6(b), the gain dynamic ranges of the OEO system are almost same for the two frequencies.

The level of  $-55$  dBm RF signals in the frequency range of 1 ~ 20 GHz were fed into the system to demonstrate the wide frequency measurement range and highly power sensitivity. As shown in Fig. 7(a), the average gain is 45 dB and maximum gain reaches 61.7 dB at frequency of 4 GHz of the system, respectively. A good curve conformity is obtained between the system gains and the RF amplifier gains. Comparing with the previous references [13], [14] using the SBS-based tunable OEO, more gain up to 30 dB could be obtained with the same input power. It is attributed to the improved sideband suppression ratio of the  $\pm 1$ st order optical sidebands by replacing the SBS gain effect with the MDR filtering effect in the PM-to-IM process. Furthermore, in the SBS-based OEO frequency measurement system, the gain dynamic range is decreased due to the system noise from high-power pump laser for SBS. The sensitivity-frequency relationship is shown in Fig. 7(b). In the measurement process, more laser power was provided at high frequencies for compensating the high-frequency loss of the system and keeping the OEO just below the oscillation threshold. The high gain of this system makes a good sensitivity as low as  $-105$  dBm. And further power sensitivity improvement can be realized by designing and fabricating a MDR filter with greater Q-factor or introducing a RF power amplifier with higher gain. The cause of gain-unflattening can be attributed to the following aspects: the changes of PM's half-wave voltages, the gain unflattening of RF amplifier and the loss imbalance of RF adapter, RF coupler and RF coaxial cable.

Based on the above principle, the received unknown signal frequency can be calculated by the difference frequency of the optical carrier from the TLS and center frequency of the MDR. The FSR of the  $\text{Si}_3\text{N}_4$  MDR-based OEO is about 10 MHz while the tuning wavelength spacing of the TLS is 125 MHz. Hence, the frequency measurement scanning step is 125 MHz. To test the frequency estimated capability, the input RF signals from 1 to 20 GHz and the step of 1 GHz with the power of  $-80$  dBm were selected. The measured results and measurement errors are shown in Fig. 8. The measurement errors are approximately  $\pm 375$  MHz, deriving from the wavelength drift of the TLS. Also, the error could be decreased by using a more fine-tuning TLS (Keysight 81699B, 0.1 pm ~ 12.5 MHz), or the wavelength stabilization feedback method.

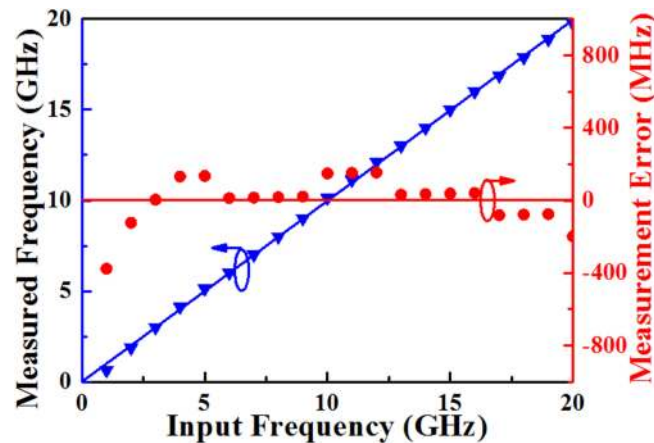


Fig. 8. The measured results (blue) and measurement errors (red).

#### 4. Conclusion

A wideband frequency measurement system for measuring the extremely low-power RF signal is proposed using a  $\text{Si}_3\text{N}_4$  micro-disk resonator-based tunable OEO. The experiment result shows that the RF signals with frequency range of 1 ~ 20 GHz and minimum input power of  $-105$  dBm can be measured. And maximum gain of 61.7 dB, frequency measurement errors of  $\pm 375$  MHz and gain dynamic range up to 75 dB were achieved. The proposed frequency measurement system has broad applications for radar monitoring and wireless communication.

#### References

- [1] J. D. McKinney, "Photonics illuminates the future of radar," *Nature*, vol. 507, no. 7492, pp. 310–311, 2014.
- [2] K. Ersan and K. Yasin, "5G mobile communication systems: Fundamentals, challenges, and key technologies," in *Proc. Smart Grids Commun. Syst.*, 2019, pp. 329–359.
- [3] Y. Ma *et al.*, "Remote sensing big data computing: Challenges and opportunities," *Future Gener. Comput. Syst.*, vol. 51, pp. 47–60, 2015.
- [4] X. Zou, B. Lu, W. Pan, L. Yan, A. Stöhr, and J. Yao, "Photonics for microwave measurements," *Laser Photon. Rev.*, vol. 10, no. 5, pp. 711–734, 2016.
- [5] C., Hao, X. Zou, and J. Yao, "An approach to the measurement of microwave frequency based on optical power monitoring," *IEEE Photon. Technol. Lett.*, vol. 20, no. 14, pp. 1249–1251, Jul. 2008.
- [6] Z. Lin *et al.*, "Wideband and low-error microwave frequency measurement using degenerate four-wave mixing-based nonlinear interferometer," *Opt. Lett.*, vol. 44, no. 7, pp. 1848–1851, 2019.
- [7] L. V. T. Nguyen and D. B. Hunter, "A photonic technique for microwave frequency measurement," *IEEE Photon. Technol. Lett.*, vol. 18, no. 10, pp. 1188–1190, May 2006.
- [8] J. S. Fandiño and P. Muñoz, "Photonics-based microwave frequency measurement using a double-sideband suppressed-carrier modulation and an InP integrated ring-assisted Mach–Zehnder interferometer filter," *Opt. Lett.*, vol. 38, no. 21, pp. 4316–4319, 2013.
- [9] X. Wang *et al.*, "Wideband adaptive microwave frequency identification using an integrated silicon photonic scanning filter," *Photon. Res.*, vol. 7, no. 2, pp. 172–181, 2019.
- [10] L. V. T. Nguyen, "Microwave photonic technique for frequency measurement of simultaneous signals," *IEEE Photon. Technol. Lett.*, vol. 21, no. 10, pp. 642–644, May 2009.
- [11] T. A. Nguyen, E. H. W. Chan, and R. A. Minasian, "Instantaneous high-resolution multiple-frequency measurement system based on frequency-to-time mapping technique," *Opt. Lett.*, vol. 39, no. 8, pp. 2419–2422, 2014.
- [12] Y. Shao, X. Han, M. Li, and M. Zhao, "RF signal detection by a tunable optoelectronic oscillator based on a PS-FBG," *Opt. Lett.*, vol. 43, no. 6, pp. 1199–1202, 2018.
- [13] G. Wang, T. Hao, W. Li, N. Zhu, and M. Li, "Detection of wideband low-power RF signals using a stimulated Brillouin scattering-based optoelectronic oscillator," *Opt. Commun.*, vol. 439, pp. 133–136, 2019.
- [14] Z. Zhu *et al.*, "Highly sensitive, broadband microwave frequency identification using a chip-based Brillouin optoelectronic oscillator," *Opt. Exp.*, vol. 27, no. 9, pp. 12855–12868, 2019.
- [15] K. Madziar and B. Galwas, "An open-loop approach to optical domain combined dual-loop optoelectronic oscillator," in *Proc. 21st Int. Conf. Microw., Radar Wireless Commun.*, May 2016, pp. 1–4.
- [16] [Online]. Available: <https://photonics.lionix-international.com/>